

Lipidomic Profiling of Bronchoalveolar Lavage Fluid Extracellular Vesicles Indicates Their Involvement in Lipopolysaccharide-Induced Acute Lung Injury

Teja Srinivas Nirujogi^a Sainath R. Kotha^b Sangwoon Chung^a
Brenda F. Reader^c Anita Yenigalla^a Liwen Zhang^d John P. Shapiro^e
Jon Wisler^f John W. Christman^a Krishnarao Maddipati^g
Narasimham L. Parinandi^a Manjula Karpurapu^a

^aDavis Heart and Lung Research Institute, Pulmonary, Critical Care and Sleep Medicine, Ohio State University Wexner Medical Center, Columbus, OH, USA; ^bComprehensive Cancer Center, Office of Health Sciences, Ohio State University, Columbus, OH, USA; ^cComprehensive Transplant Center, Ohio State University Wexner Medical Center, Columbus, OH, USA; ^dProteomics Shared Resources, Mass Spectrometry and Proteomics Facility, Ohio State University, Columbus, OH, USA; ^eDepartment of Internal Medicine, Nephrology, Ohio State University, Columbus, OH, USA; ^fDivision of Trauma and Critical Care, Department of Surgery, Ohio State University, Columbus, OH, USA; ^gDepartment of Pathology, Lipidomics Core Facility, Wayne State University, Detroit, MI, USA

Keywords

Acute lung injury · Inflammation · Extracellular vesicles · Polyunsaturated fatty acids · Macrophage

Abstract

Emerging data support the pivotal role of extracellular vesicles (EVs) in normal cellular physiology and disease conditions. However, despite their abundance, there is much less information about the lipid mediators carried in EVs, especially in the context of acute lung injury (ALI). Our data demonstrate that C57BL/6 mice subjected to intranasal *Escherichia coli* lipopolysaccharide (LPS)-induced ALI release, a higher number of EVs into the alveolar space, compared to saline-treated controls. EVs released during ALI originated from alveolar epithelial cells, macrophages, and neutrophils and carry a diverse array of lipid mediators derived from ω -3

and ω -6 polyunsaturated fatty acids (PUFA). The eicosanoids in EVs correlated with cellular levels of arachidonic acid, expression of cytosolic phospholipase A2, cyclooxygenase (COX), lipoxygenase (LOX), and cytochrome epoxygenase p450 proteins in pulmonary macrophages. Furthermore, EVs from LPS-toll-like receptor 4 knockout (TLR4^{-/-}) mice contained significantly lower amounts of COX and LOX catalyzed eicosanoids and ω -3 PUFA metabolites. More importantly, EVs from LPS-treated wild-type mice increased TNF- α release by macrophages and reduced alveolar epithelial monolayer barrier integrity compared to EVs from LPS-treated TLR4^{-/-} mice. In summary, our study demonstrates for the first time that the EV carried PUFA metabolite profile in part depends on the inflammatory status of the lung macrophages and modulates pulmonary macrophage and alveolar epithelial cell function during LPS-induced ALI.

© 2022 The Author(s).
Published by S. Karger AG, Basel

Introduction

The pathophysiology of acute lung injury (ALI) and a severe form of ALI, acute respiratory distress syndrome (ARDS), is orchestrated primarily by the complex interaction of pulmonary macrophages, microvascular endothelial, and alveolar epithelial cells. Macrophage-derived chemokines recruit neutrophils that transmigrate across the epithelium and release reactive oxygen species, proteases, and extracellular traps that play a pivotal role in host defense and cause inflammation. Migration of inflammatory monocytes into the alveoli results in alveolar epithelial and microvascular endothelial cell damage leading to fluid extravasation and hypoxemia [1]. Further, activated platelets form aggregates with polymorphonuclear leukocytes, monocytes, and the red blood cells release cell-free hemoglobin, which exacerbates inflammation via oxidant-dependent mechanisms. Therapeutic strategies using β 2-adrenergic receptor agonists, statins, vitamin D3, and mesenchymal stem cells that target the cellular mediators at different levels have not effectively controlled the ALI/ARDS disease outcomes [2–5]. The possible reason for the failure of these approaches could be due to the heterogeneous and complex mechanisms underlying the disease. Thus, identifying the complex interplay of cellular events that regulate ALI/ARDS is essential for developing effective therapies.

Compared to other cell types, macrophages are involved in the metabolism and trafficking of lipids to a greater extent, as they acquire lipids from phagocytic activity. Multiple studies support the pivotal role of lipid mediators in inflammatory pathologies and activation of both innate and adaptive immunity [6–8]. ALI is associated with increased release of arachidonic acid (AA) from the cell membrane phospholipids by the phospholipase A₂ (PLA₂) [9, 10]. While different classes of PLA2 operate in lipid metabolism, class IV cytosolic PLA2 (cPLA2) is the major source for cellular-free AA levels [11]. AA is further metabolized by the enzymatic action of different cyclooxygenase (COX), lipoxygenase (LOX), and cytochrome p450 epoxygenases/ ω -hydroxylase pathways or via nonenzymatic-free radical mechanisms [12]. The COX, LOX, and CYP450 enzymes generate bioactive lipids that can act as signaling molecules. The COX pathway comprises of enzymes COX-1 and COX-2, and downstream enzymes that generate prostaglandins (Prostaglandin E2 [PGE₂], PGD₂, and PGF₂ α), prostacyclin (PGI₂), and thromboxanes (TXA₂), collectively referred to as “prostanoids.” The LOX pathway consists of 5-LOX, 8-LOX, 12-LOX, and 15-LOX (12/15-LOX in mice) en-

zymes and their catalytic products, leukotrienes (LTA₄, leukotriene B₄ [LTB₄], LTC₄, LTD₄, and LTE₄), lipoxins (LXA₄, LXB₄), and 8, 12 or 15-hydroperoxyeicosatetraenoic acid compounds. The cytochrome p450 pathway comprises two enzymes, CYP450 epoxygenase and CYP450 ω -hydroxylase, which generate epoxyeicosatrienoic acid (EET) and hydroxyeicosatetraenoic acid compounds (HETEs), respectively from polyunsaturated fatty acids (PUFAs). Although leukotrienes and prostanoids are frequently linked with inflammation, the recently identified proresolving lipoxins from AA, ω -3 PUFA-derived resolvins, protectins, and maresins are implicated in the resolution of inflammation and restoration of tissue homeostasis [13–15]. In the setting of inflammatory pathologies, PGE₂ and LTB₄ were shown to act as neutrophilic chemo attractants whereas the lipoxins, D and E series resolvins, and maresins to aid in the resolution of inflammation, named as specialized proresolving mediators generated from essential FA, including AA, eicosa-pentaenoic acid (EPA), and docosahexaenoic acid (DHA) [14]. The lipoxins are synthesized from leukocyte-derived 5-LOX and platelet-derived 12-LOX from AA as substrate. Lipoxins are also synthesized by transcellular metabolism of AA by epithelial cell or monocyte-derived 15-LOX and leukocyte-derived 5-LOX in the extravascular compartments [16].

Since their discovery 30 years ago, there is mounting evidence of the role of extracellular vesicles (EVs) in regulating normal and disease physiology. EVs are lipid bilayer membrane-bound vesicles released extracellularly, which originate from the cellular endosomal system or plasma membrane [17, 18]. Based on their cellular origin and size, EVs are classified as small, medium, and large EVs. Small EVs ~40–100 nm, originating from endosomal microvesicular bodies are the focus of the current study. Microvesicles (MVs) ~100–1,000 nm, originate from plasma membrane and apoptotic bodies \geq 1 μ m, originate from cells undergoing apoptosis [19]. EVs transfer membrane proteins or other bioactive cargo, including nucleic acids, lipids, and peptides to the recipient cells [20–23]. The lipid composition of EVs depends largely on their cellular source and microenvironment [23, 24]. However, bilayer lipid membranes of EVs are enriched in sphingomyelin, cholesterol, phosphatidylserine, and glycosphingolipids compared to their parent cells, offering more structural stability [20]. Thus, EVs could potentially increase the stability of their biological cargo that mediate intercellular communication. EV carried micro-RNAs (miRs) were shown to regulate the inflammatory signaling pathways during ALI/ARDS. For example, miR-466

released into BALF of ARDS mice exacerbated pulmonary inflammation through the NLRP3 inflammasome activation [25]. In contrast, the plasma membrane-generated MVs from lipopolysaccharide (LPS) or *Klebsiella pneumoniae*-induced ALI in mice carried miR-223/142, which suppressed NLRP3 inflammasome activation [26]. Epithelial cell-derived MV from acid-induced ALI mice are enriched in miR-17 and miR-221 that promoted β 1 integrin recycling and macrophage migration and recruitment during lung inflammation [27]. EVs from LPS-stimulated rat alveolar epithelial cells initiated pro-inflammatory signaling in alveolar macrophages by the activation of the NF- κ B pathway by shuttling miR-92a-3p, and inhibition of miR-92a-3p abolished pro-inflammatory/NF- κ B signaling [28]. Similarly, MVs from mice subjected to LPS-induced ALI contained significant amounts of TNF- α and lower amounts of IL-1 β /IL6, compared to healthy control mice. Furthermore, culture of MLE-12 cells with MVs from LPS-treated ALI mice-induced expression of epithelial intercellular adhesion molecule-1 and keratinocyte-derived cytokine release and induced neutrophilic infiltration when delivered intratracheally into mice [29]. To our knowledge, there are no published studies that investigated the lipid constituents of EVs from lung injury patients or animal models. In the current study, we demonstrate that LPS-induced ALI causes an increase in the release of EVs into the alveolar space, packaged with ω -6 and ω -3 PUFA metabolites. We have specifically characterized the role of 40–100-nm size EVs and their lipid cargo in regulating LPS-induced ALI using the toll-like receptor 4 (TLR4^{-/-}) mice.

Materials and Methods

Mouse Models of LPS-Induced ALI

Wild-type C57BL/6 (WT-Stock no. 000664) and TLR4^{-/-} (Stock no. 029015) mice purchased from the Jackson Research Laboratories (Bar Harbor, ME, USA) and maintained in the pathogen-free vivarium. Eight to twelve-week-old mice were used for all the animal experiments, conducted following protocols approved by the Institutional Animal Care and Use Committee of The Ohio State University. *Escherichia coli* LPS Serotype O55:B5 S-form, dissolved in sterile saline was delivered through intranasal insufflation into anesthetized WT or TLR4^{-/-} mice (4 mg/kg in 25- μ L saline). Control mice received an equal volume of saline. After 6 h, 3 days, and 15 days of LPS treatment, mice were euthanized with ketamine/xylazine, trachea was cut open, BALF was collected by instilling 1-mL sterile saline three times and aspirating. Aspirated BALF was centrifuged at 300 g to separate cells, and the supernatant was used for TNF- α , IL6, extravasated protein measurements, and EV isolation. Cytokine release was analyzed using R&D Systems ELISA kits for mouse TNF- α (catalog no. MTA00B) and IL-6

(catalog no. M6000B) following the protocols supplied by the manufacturer. Lung wet dry ratios and histological changes were determined as described previously [30].

Isolation of EVs

EVs were isolated by ultracentrifugation as per the published protocol [31]. In brief, BALF from each mouse was centrifuged sequentially at 300 g, 2,000 g, and 10,000 g to separate cells, apoptotic bodies, and MV. MV-depleted BALF was filtered through 0.22- μ m syringe filters, centrifuged at 100,000 g for 6 h at 4°C using TLA100 fixed angle rotor on Beckman Coulter ultracentrifuge. The EV pellet was resuspended in 1-mL PBS, centrifuged at 100,000 g, before final reconstitution in PBS for downstream analyses.

Size Determination and Transmission Electron Microscopy

Sizes of different EVs in BALF were determined by nanoparticle analysis using NanoSight at OSU Comprehensive Cancer Center Flow cytometry facility. Mean size, particle numbers were compared between different BALF samples/vesicles isolated from individual mice. Photomicrographs of EVs were captured by negative staining using FEI Tecnai G2 Biotwin Transmission electron microscope at OSU Comprehensive Cancer Center-Campus Microscopy and Instrumentation facility.

Cellular Source of EVs

Cellular source of EVs was determined by flow cytometry using CD9 Exo-Flow capture beads (System Biosciences; Palo Alto, CA, USA) as per manufacturers' instructions. EVs were attached to CD9 labeled Exo-Flow beads at 4°C, for 16 h, and stained with F4/80-APC, CD31-FITC, CD326-PE, and Ly6G-BV421 (eBioscience) antibodies, and analyzed on BD LSR Fortessa Flow Cytometer at OSU Flow cytometry core facility. Data were analyzed using FlowJo.

Analysis of EV Lipid Mediators

EV eicosanoids and bioactive lipid mediators were isolated by Solid Phase Extraction on C18 columns and analyzed as described previously using liquid chromatography-mass spectrometry at Lipidomics Core Facility, Wayne State University, Detroit [32].

Isolation of Lung Macrophages

Total lung leucocytes were isolated by digesting mouse lungs with collagenase and DNase as described previously [33]. From these, total lung macrophages were isolated by adherence purification, grown on 12-well plates for EV uptake and TNF- α release assay. In a parallel set of experiments, lung macrophages were washed with sterile PBS and resuspended in PBS or radio immune precipitation assay buffer for analyzing fatty acid composition, immunoblotting of PUFA metabolic proteins.

Analysis of Fatty Acid Composition

Total lipids from alveolar macrophages were extracted and analyzed by HPLC using appropriate internal standards as described previously [34].

Western Blot Analysis

Total lung macrophages or MVs/EVs were lysed in radio immune precipitation assay lysis buffer (Cell Signaling Technologies, Danvers, MA, USA) with 1 \times protease inhibitor cocktail (Thermo Fisher, Waltham, MA, USA). Cell lysates containing 10 μ g of total protein were electrophoresed on 4%–20% SDS-PAGE gradient

gels, transferred onto PVDF membranes, and immunoblotted with cPLA2, COX-1, COX-2, 5, 12/15-LOX and CYP450 antibodies, and HRP-conjugated secondary antibodies. Expression levels of proteins were detected using a streptavidin-HRP chemiluminescence detection system (ThermoFisher, Waltham, MA, USA).

cPLA2 Activity Assay

Enzymatic activity of cPLA2 in lung macrophages was assayed using Arachidonoyl Thio-PC as substrate in the cPLA2 assay kit (Cayman Chemical; Ann Arbor, MI, USA) as per the manufacturers' instructions. Specific activity was expressed as μmol of Arachidonoyl Thio-PC hydrolyzed per min per mg cellular protein.

Analysis of EV Uptake

EV were labeled with PKH26 and purified on sucrose gradient ultracentrifugation as per the manufacturers' instructions (Sigma-Aldrich, St. Louis, MO, USA). PKH26-labeled EV (10^9 /well) were added to 5×10^3 primary mouse alveolar epithelial cells (Cell Biologics, Chicago, IL, USA) plated on collagen type-I coated 96-well plates and grown to 100% confluence, at 37°C for 16 h. Similarly, PKH26-labeled EVs were added to 5×10^3 lung macrophages, incubated further for 16 h on 96-well plates. Next, the cells were washed gently with $1 \times$ HBSS, incubated with CD9-Exo-Flow capture beads (System Biosciences, Palo Alto, CA, USA) for 1 h to remove EVs loosely attached to cell membranes. Cells were washed twice with $1 \times$ HBSS and uptake of EVs was quantified by fluorescence plate reader (530 nm/567 nm) and expressed as relative fluorescence units (RFU). Cells incubated in presence of unlabeled EVs were included to measure baseline fluorescence.

Alveolar Epithelial Cell Barrier Function

To assess monolayer permeability, mouse primary alveolar epithelial cells were cultured on 24-well collagen-coated transwell inserts (0.4- μm pore size) to 100% confluence. EVs were added to transwells along with 100 $\mu\text{g}/\text{mL}$ FITC-dextran (10 kDa, Invitrogen). Flux of FITC-dextran into bottom wells was measured using 100 μL medium from the basolateral chamber after 0 and 16 h of EV addition. An equal volume of culture medium was added to the chamber to compensate for the reduction in volume due to sampling. Fluorescence was measured using a plate reader at 492/520 nm excitation/emission.

Statistical Analysis

All data are expressed as mean \pm SEM, $n = 5$ in each group, repeated three times. Differences between two experimental groups were compared with Student's *t* test and comparisons among the four groups were performed using ANOVA with a post hoc Bonferroni correction test, using Graphpad Prism 9.0. $n = 4$ mice in each group processed separately for lipidomics analyses, false discovery rate threshold set at 1%. Lung injury parameters were assayed using $n = 5$ mice in the control group, and $n = 8$ mice in the LPS group, representative data sets were presented. *p* value < 0.05 was considered significant.

Results

LPS Increases Release of EVs into BALF

A mouse model of LPS-induced ALI was used to delineate the role of BALF EV lipid mediators on lung in-

flammation and injury. Nanoparticle tracking analysis of total cell-free BALF from control mice at 6 h, 3 and 15 days post treatment showed a mixed population of vesicles from 40 to 500 nm size (Fig. 1a – total BALF). As expected, the MV fraction contained vesicles ranging in size from 200 to 500 nm (Fig. 1a – MV). MV-depleted supernatant was centrifuged at 100,000 *g* for 6 h to pellet EVs. The size of EVs ranged from 40 to 160 nm, and the most frequently represented EV size was 100–140 nm (Fig. 1a – EV). The number of EVs in BALF was significantly higher after LPS treatment (Fig. 1b). In addition, the size of EVs was found to be in the 100–140 nm range determined by transmission electron microscope (Fig. 1c). Immunoblotting confirmed the presence of CD9 and CD63 proteins indicating the endosomal origin of EVs (Fig. 1d). As expected, BALF levels of TNF- α were significantly elevated at 6 h and 3 days, which decreased to basal levels after 15 days of the LPS challenge (Fig. 1e). The amount of phospholipids per milligram protein in EV-depleted BALF was significantly lower than that of EVs, indicating that most of the phospholipids were packaged in EVs (Fig. 1f).

EVs Carry Diverse Array of Lipid Mediators

Total lipids from the EVs were analyzed by liquid chromatography in conjunction with mass spectrometry to characterize the lipid cargo. Intranasal LPS-induced ALI shows acute-inflammatory phase up to 3 days characterized by increased IL6, TNF- α , neutrophilic influx, and pulmonary vascular leak, which resolves by 9 days [35]. EVs from inflammatory and resolution phases of ALI were enriched with a wide array of PUFA metabolites, bioactive eicosanoids resulting from the enzymatic and nonenzymatic conversion of AA, DHA, and EPA (Fig. 2a, b; online supplementary Table 1 (see www.karger.com/doi/10.1159/000522338 for all online suppl. material). Both pro-inflammatory and pro-resolution eicosanoids are elevated in the acute-inflammatory phase (3 days post-LPS), which decreased in the resolution phase (15 days post-LPS) of ALI. LOX metabolites of AA, including LTB4, 5-HETE, 12-HETE, 15-HETE, and COX metabolites (PGE₂, PGD₂, PGF₂ α , TXB₂), were the most abundant eicosanoids packaged in EVs. Similarly, the EPA-derived 5, 11, 12, 15, and 18-hydroxyeicosapentaenoic acid (5, 11, 12, 15, and 18-HEPE) and DHA-derived Resolvin D6 (RvD6), 8-oxo-Resolvin D1 (8-oxoRvD6) are enriched in EVs 3 days post-LPS injury. In addition, EVs also contained inactive prostanoid metabolites and stereoisomers of PGE1, such as 15-keto-PGE1 and 15R-PGE1. Furthermore, metabolic intermediates of PGE₂,

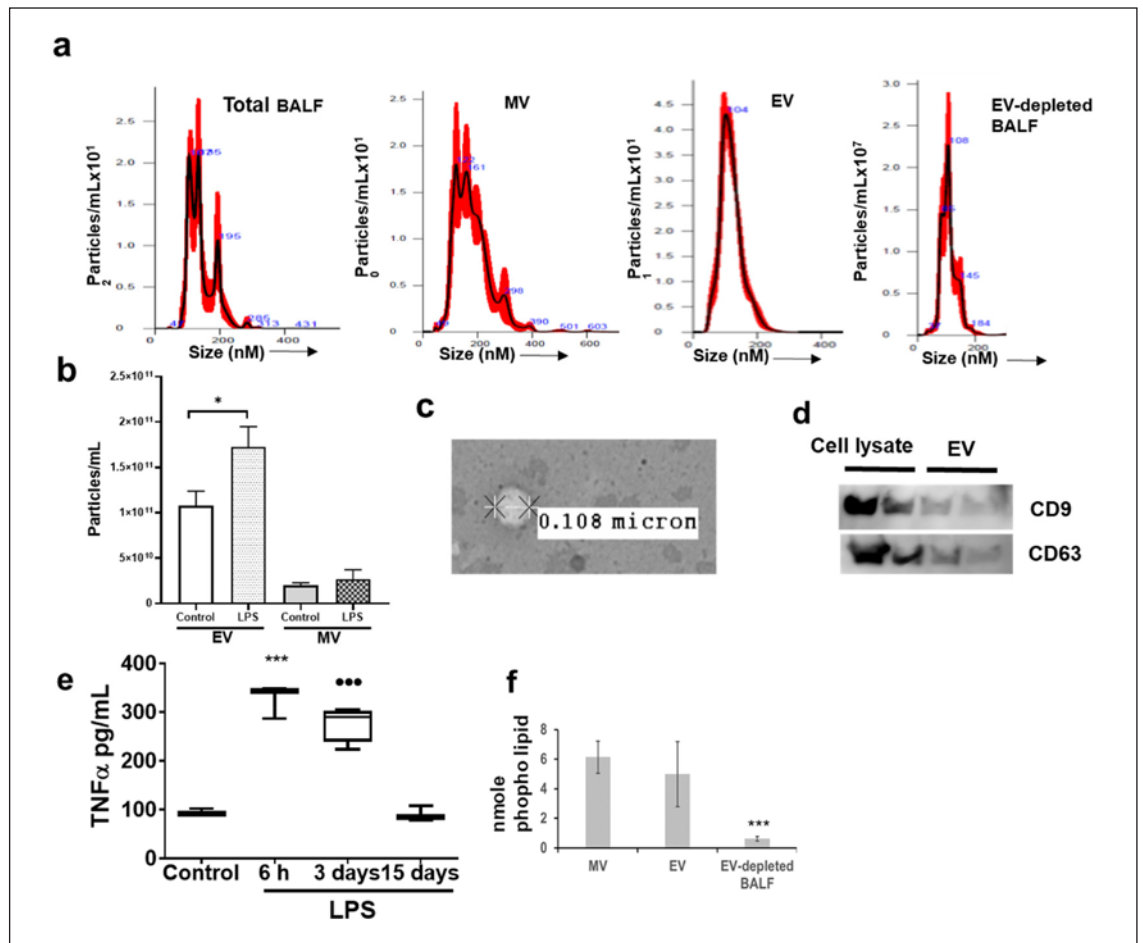


Fig. 1. Characterization of EVs from mouse BALF. BALF was subjected to sequential centrifugation to separate cells, apoptotic bodies, MVs, and EVs. **a** Size distribution of vesicles in total BALF, MVs, EVs, and EV-depleted supernatant was assayed by NTA. **b** Difference in release of EVs into BALF from control (saline) and LPS-treated mice. **c** Determination of EV size by transmission electron microscopy. **d** Expression of EV marker proteins CD9, CD63 in EVs. **e** TNF- α levels in EV-depleted BALF in saline and

LPS treatment after 6 h, 3, and 15 days. **f** Comparison of phospholipid content of MVs, EVs, and EV-depleted BALF. The error bars represent the mean \pm SEM from five mice in each group. Statistical difference between different treatments calculated by one-way ANOVA with Bonferroni correction. **b** $*p \leq 0.05$ LPS versus saline control (**e**), $***/\bullet\bullet\bullet p \leq 0.001$ LPS versus saline control. **f** $***p \leq 0.001$ EV or MV versus EV-depleted BALF. NTA, nanoparticle tracking analysis.

PGD2, PGF2 α , TXB2 are enriched in EVs on day 3 of LPS-induced lung inflammation and decreased by 15 days. The essential fatty acid LA-derived metabolites, 9- and 13 hydroxyoctadecadienoic acids (9-HODE and 13-HODE), and their derivatives 9- and 13-oxo-octadecadienoic acid (9-oxoODE and 13-oxoODE), generated by NAD⁺ dependent dehydrogenase followed a similar trend with other lipid mediators. Saline treated or 15 days post-LPS injured mice contained significantly lower lipid mediators of all classes.

To determine if disruption of LPS-induced signaling alters EV lipid cargo, we have analyzed TLR4^{-/-} mice sub-

jected to LPS-induced ALI (4 mg/kg i.n.). As anticipated, there was a marked decrease in BALF IL6 and TNF- α levels, protein, and lung wet to dry ratios (indicating vascular leak and pulmonary edema) than WT mice (Fig. 3a-d). Interestingly, the total EV numbers were similar between TLR4^{-/-} and WT mice (Fig. 3f). Furthermore, the BALF EVs were derived from epithelial cells (CD326+), neutrophils (Ly6G+), and macrophages (F4/80+) in decreasing order (Fig. 3e). On the other hand, no pulmonary microvascular endothelial cell-derived EVs (CD31+) were detected in BALF, and the epithelial-derived EVs increased by $\sim 50\%$ in both WT and TLR4^{-/-} ALI mice.

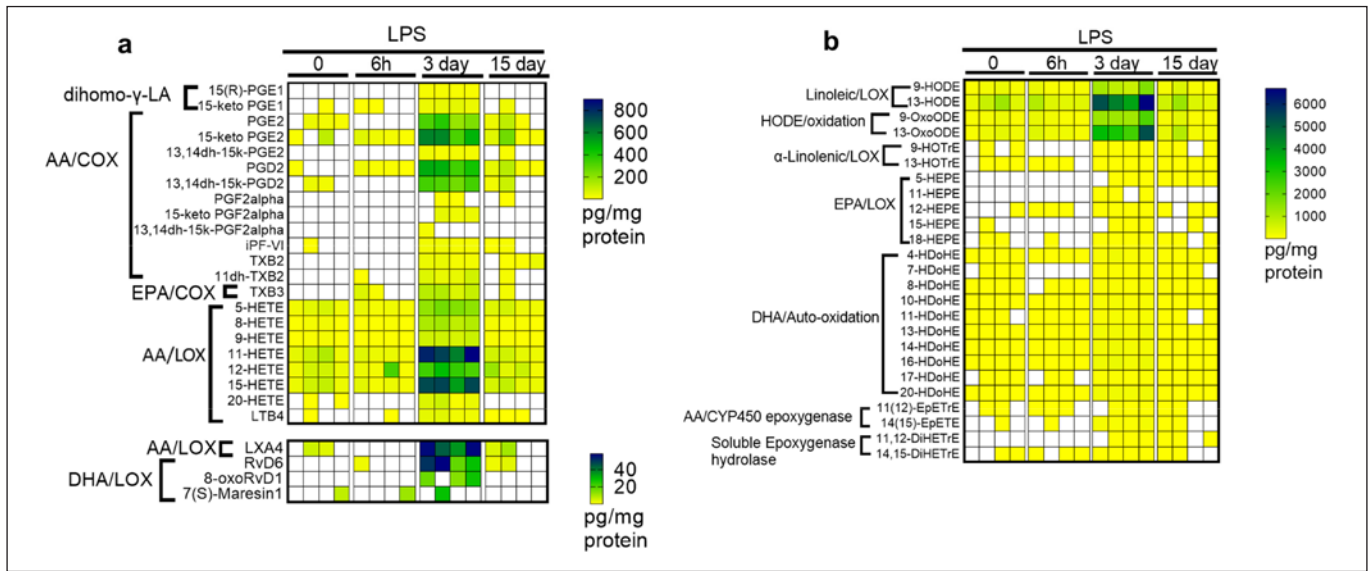


Fig. 2. BALF EVs from LPS-treated mice carry a diverse array of ω -6 and ω -3 PUFA metabolites. WT mice were treated with LPS or saline (i.n.), and BALF was collected after 6 h, 3, and 15 days later. EVs from BALF of individual animals ($n = 4$) were isolated by ultracentrifugation and confirmed by size determination. **a**, **b** The relative amount of AA, EPA, DHA, and LA-derived metabo-

lites from enzymatic action of COX, LOX, CYP450, and nonenzymatic lipid peroxidation were determined by LC-MS. Heat map constructed using Graphpad Prism v9.0. Scale bar represents picogram of metabolite per milligram of EV protein. Samples with no detectable metabolites are in white.

In addition, the neutrophil and macrophage-derived EVs were significantly lower in $TLR4^{-/-}$ compared to WT mice subjected to ALI, which agrees with the lung tissue injury severity and neutrophilic infiltration (Fig. 3g). Thus, as expected, the $TLR4^{-/-}$ mice were hypo-responsive to LPS-induced inflammation, as they lack TLR4, the primary transducer of LPS-induced signaling [36, 37].

AA Metabolome in EVs

EVs from LPS-challenged $TLR4^{-/-}$ mice contained significantly lower amounts of both pro-inflammatory and pro-resolution eicosanoids compared to LPS-challenged WT mice (Fig. 4a–e). LPS is a known activator of the TLR4-NF- κ B-COX-2 signaling axis. The EVs from $TLR4^{-/-}$ ALI mice are devoid of AA/COX metabolites, including prostaglandins and thromboxane B2/B3, possibly because of disruption of the TLR4-NF- κ B-COX signaling axis (Fig. 4a). Similarly, the pro-inflammatory AA/LOX metabolites 5-HETE, 12-HETE, and 15-HETE and the proresolving lipid mediator lipoxin A4 (LXA4) are significantly lower in $TLR4^{-/-}$ EVs compared to WT EVs (Fig. 4b–e). Also found in lower amounts in $TLR4^{-/-}$ EVs were the inactive COX metabolites of AA, including 15-Keto-PGE1, 15-keto-PGE₂, and 13, 14dh-15k-PGD2 (Fig. 4a). The COX metabolite, 15-keto PGF2- α , which

causes contraction of pulmonary arteries, was high in the EVs of the WT-LPS mice, whereas the same was undetectable in the $TLR4^{-/-}$ LPS mice (Fig. 4a). Similarly, thromboxane B2 (TXB2) and the nonenzymatic oxidized species of AA and isoprostane iPF-VI (a biomarker of lipid peroxidation) levels were higher in the BALF EVs of WT-ALI mice. In contrast, the same was absent in the EVs from lung injured $TLR4^{-/-}$ mice (Fig. 4a).

DHA and EPA Metabolome in EVs

DHA-derived metabolites, including hydroxydocosahexaenoic acids (4-HDoHE, 10-HDoHE, and 20-HDoHE), were selectively packaged in the WT EVs, 3 days post-LPS challenge (Fig. 5a–c). However, the BALF EVs from LPS-treated $TLR4^{-/-}$ mice harbored negligible amounts of these ω -3 PUFA metabolites. Notably, the DHA-derived D-series resolvins, including resolvin D1, D6, and Maresin 1, were packaged more in WT EVs than the $TLR4^{-/-}$ EVs (Fig. 5d). The EPA-derived 15-HEPE followed similar trends with other ω -6 and ω -3 and PUFA metabolites (Fig. 5e). In summary, BALF EVs of the LPS-challenged WT mice contained increased amounts of DHA and EPA-derived metabolites, which were either attenuated or undetectable in the LPS-challenged $TLR4^{-/-}$ mice (Figs. 4, 5).

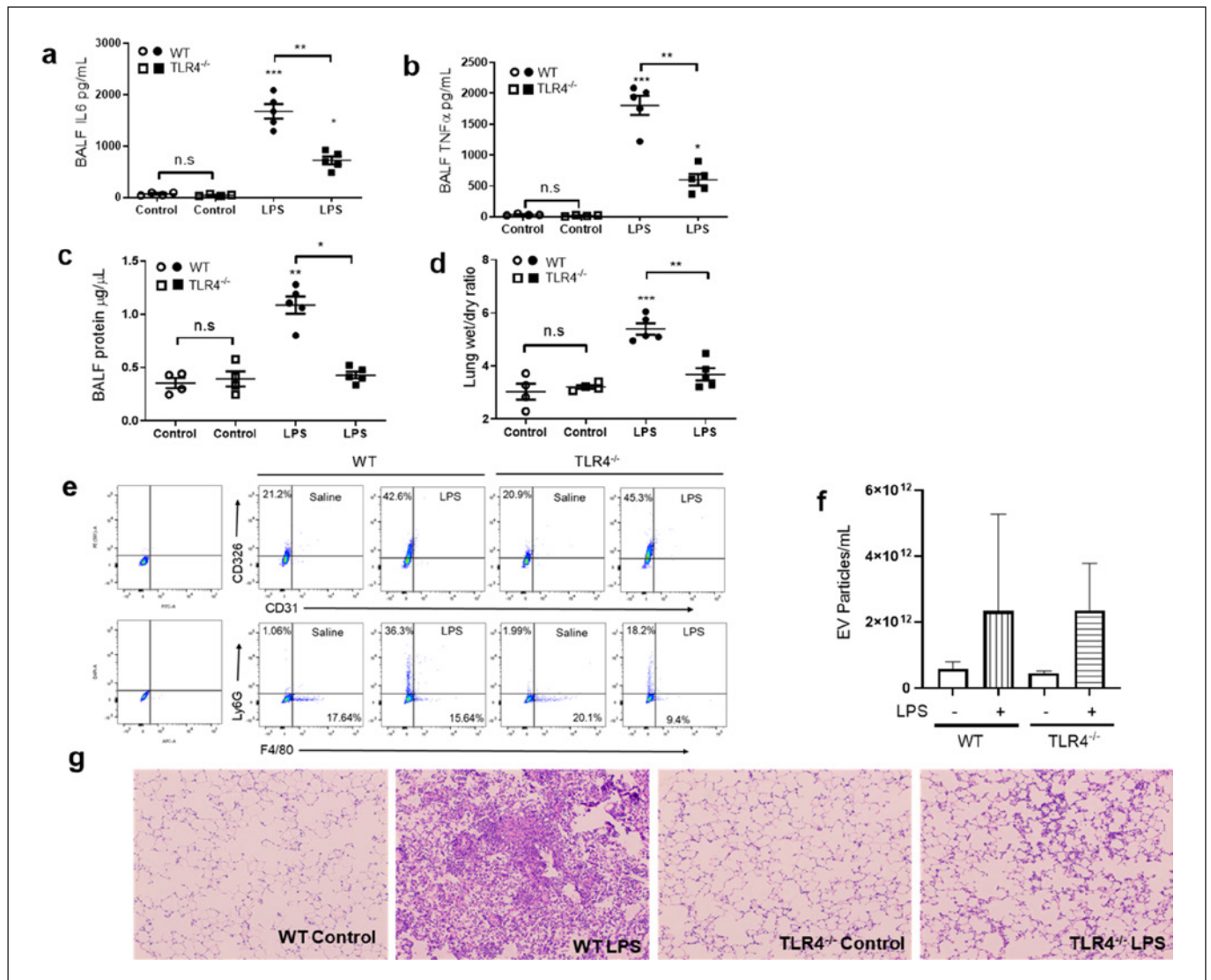


Fig. 3. TLR4^{-/-} mice are resistant to LPS-induced ALI, release lower number of macrophage and neutrophil-derived EVs into BALF. WT and TLR4^{-/-} mice were treated with LPS or saline (i.n.). After 3 days of LPS challenge mice were euthanized, and lung injury severity was determined by measuring BALF levels of IL6 (**a**), TNF-α (**b**), extravasated protein (**c**), and lung wet to dry ratios (**d**). BALF EVs were attached to CD9-Exo-Flow capture beads, stained with F4/80-APC, CD31-FITC, CD326-PE, Ly6G-BV421, and analyzed on BD LSR Fortessa Flow Cytometer (**e**). Data were analyzed using FlowJo v10.8.1. The total number of BALF EVs compared between

WT and TLR4^{-/-} mice, subjected to control or LPS-induced ALI (**f**). Lung sections of WT and TLR4^{-/-} mice subjected to control or LPS-induced ALI were stained with H & E. Representative sections showing lung injury and neutrophilic infiltration (**g**). **a-d** Error bars represent mean ± SEM from 5 mice in each group. Statistical difference calculated by one-way ANOVA with Bonferroni correction. **a, b, d** *** $p \leq 0.001$ WT LPS versus WT-saline control; ** $p \leq 0.01$ WT-LPS versus TLR4^{-/-}-LPS. **c** ** $p \leq 0.01$ WT-LPS versus WT-saline control, * $p \leq 0.05$ WT-LPS versus TLR4^{-/-}-LPS.

Macrophage Fatty Acid Composition and Metabolic Protein Expression

As the content of total esterified FAs in the membrane phospholipids correlate with downstream metabolism in cells, we have determined the molar concentration of the ω-6 and ω-3 fatty acids and the expression levels of PUFA

catalytic proteins in lung macrophages. Our data show that the enzymatic activity of cPLA2 (assayed in the presence of sPLA2 and iPLA2 inhibitors) was significantly higher in total lung macrophages from LPS-treated WT than TLR4^{-/-} mice (Fig. 6a). Similarly, lung macrophages from LPS-challenged WT mice showed increased expres-

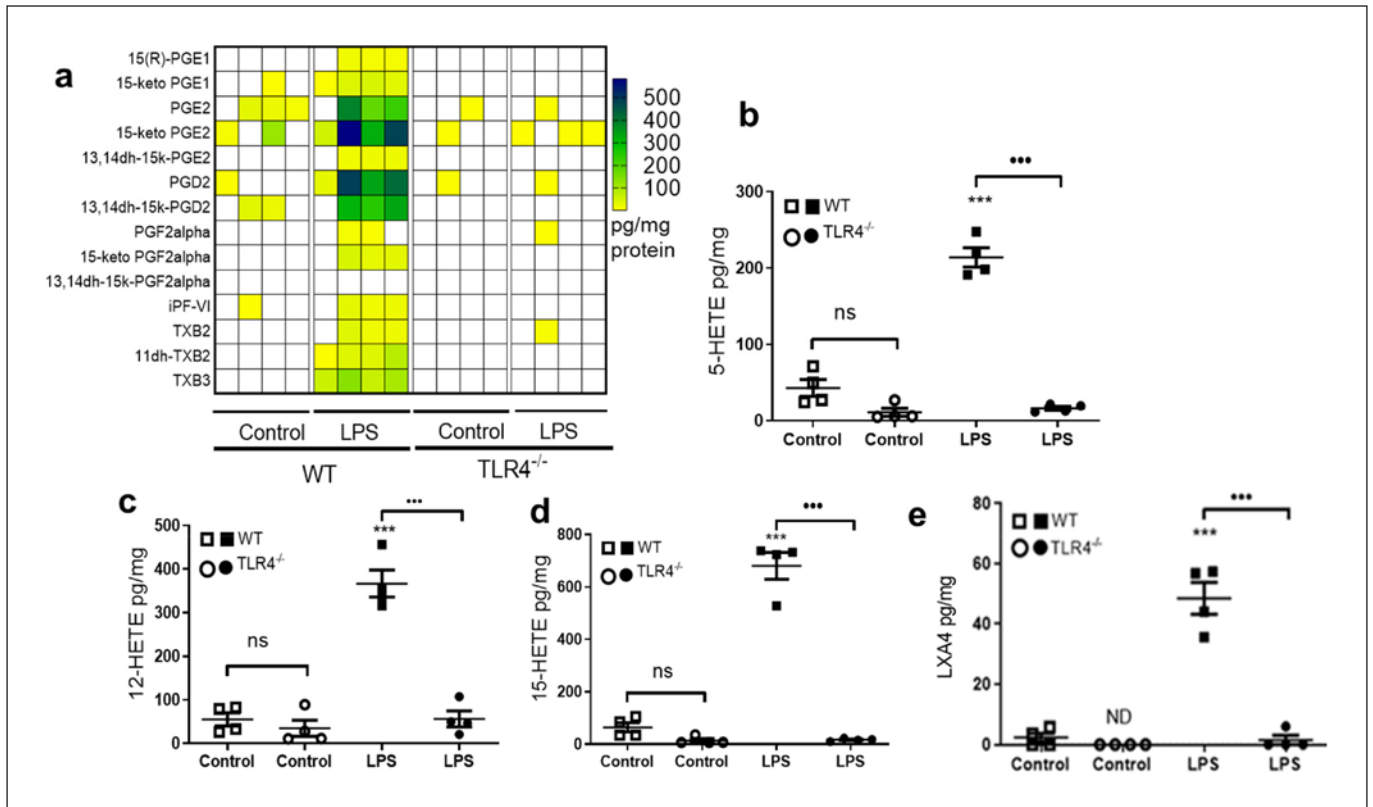


Fig. 4. BALF EVs from TLR4^{-/-} mice are devoid of AA-derived eicosanoids. EVs were isolated from saline or LPS-treated WT and TLR4^{-/-} mice and analyzed by LC-MS. COX metabolites in EVs from saline or LPS-treated mice (**a**). Similarly, LOX metabolites were determined in EVs isolated from saline or LPS-treated WT and TLR4^{-/-} mice, showing levels of 5-HETE (**b**), 12-HETE (**c**), 15-HETE (**d**), and LXA4 (**e**). $n = 4$ mice in each group, EVs from each mouse processed separately. Heat map constructed using

Graphpad Prism v9.0 and statistical differences calculated by one-way ANOVA with Bonferroni correction. **b-e** *** $p \leq 0.001$ WT LPS versus WT-saline control; ** $p \leq 0.01$ WT-LPS versus TLR4^{-/-}-LPS. Scale bar represents picogram of metabolite per milligram of EV protein. Samples with no detectable metabolites are in white. 5-HETE, 5-hydroxyeicosatetraenoic acid; 12-HETE, 12-hydroxyeicosatetraenoic acid; 15-HETE, 15-hydroxyeicosatetraenoic acid; LXA4, lipoxin A4.

sion of cPLA2, COX-2, and 5-LOX proteins compared to TLR4^{-/-} lung macrophages (Fig. 6b). Expression levels of 12 and 15-LOX proteins increased moderately in response to LPS in WT lung macrophages. In addition, the total cellular fatty acid composition (% AA and EPA) in LPS-treated WT lung macrophages was higher than TLR4^{-/-} lung macrophages (Fig. 6c, e), whereas the DHA content was similar in both strains of mice (Fig. 6d). In conclusion, pulmonary macrophage PUFA content and metabolizing proteins correlate with lower ω -6 and ω -3 PUFA metabolites in EVs from TLR4^{-/-} mice (Fig. 4, 5, 6a-e).

Lipid Mediators in EVs Alter Pulmonary Macrophage and Alveolar Epithelial Cell Function

As the lipid mediators were known to initiate cellular signaling and alter their function, we sought to determine

the role of EV carried lipid mediators in influencing mouse lung macrophages and alveolar epithelial cell monolayer barrier function using in vitro assays. Both the alveolar epithelial cells and lung macrophages internalized PKH26-labeled EVs, measured by arbitrary RFU (Fig. 7a, b). As seen by relative fluorescence intensity, there was no difference in uptake of saline or LPS generated EVs from WT or TLR4^{-/-} mice by the macrophages and alveolar epithelial cells (Fig. 7a, b). As expected, pretreatment with the EV uptake inhibitors Nystatin (50 μ g/mL) and cytochalasin D (10 μ g/mL) have decreased the EV uptake by 50%–60% compared to solvent control (Fig. 7a, b). Relative fluorescence intensity of alveolar epithelial cells and macrophages incubated with unlabeled EVs showed RFU values lower than 5 and 20, respectively. WT-LPS EVs (10^{11} /well) disrupted epithelial cell

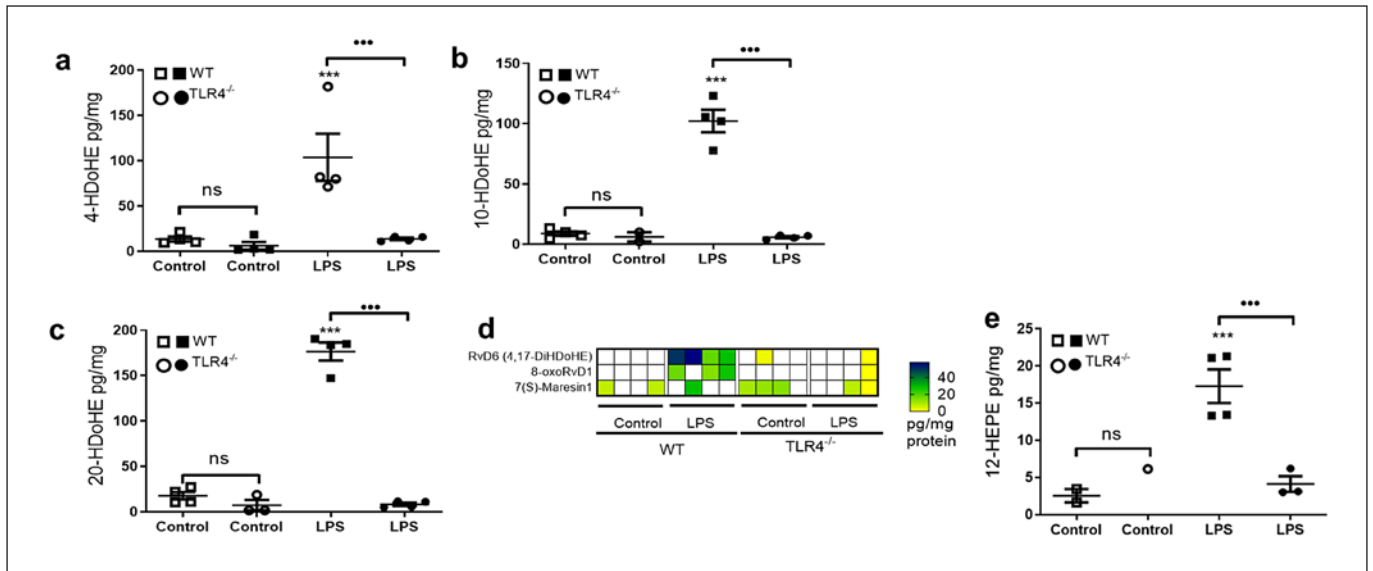


Fig. 5. BALF EVs from TLR4^{-/-} mice are devoid of DHA and EPA-derived lipid mediators. EVs were isolated from saline or LPS-treated WT and TLR4^{-/-} mice and analyzed for the presence of DHA auto-oxidation metabolites and DHA-derived resolvins. Levels of 4-HDoHE (a), 10-HDoHE (b), 20-HDoHE (c). Heat map showing relative levels of Resolvin D6, 8-oxoResolvin D1, and Maresin 1 (d). EPA-derived 12-HEPE (e). *n* = 4 mice in each group, EVs from each mouse processed separately. Statistical difference

calculated by one-way ANOVA with Bonferroni correction. a-e ****p* ≤ 0.001 WT LPS versus WT-saline control; •••*p* ≤ 0.001 WT-LPS versus TLR4^{-/-}LPS. Scale bar represents picogram of metabolite per milligram of EV protein. Samples with no detectable metabolites are in white. 4-HDoHE, 4-Hydroxydocosahexaenoic acid; 10-HDoHE, 10-Hydroxydocosahexaenoic acid; 20-HDoHE, 20-Hydroxydocosahexaenoic acid; 12-HEPE, 12-hydroxyeicosapentaenoic acid.

monolayer integrity resulting in increased FITC-dextran flux into the bottom chamber of trans wells (Fig. 7c). In contrast, the exact EV numbers from WT-saline or TLR4^{-/-} saline or TLR4^{-/-} LPS-treated mice had no negative impact on the alveolar epithelial cell monolayer integrity (Fig. 7c). Furthermore, WT-LPS EVs (10¹¹/well) also increased TNF-α release by lung macrophages compared to WT-saline or TLR4^{-/-} EVs (Fig. 7d). Nystatin and cytochalasin D prevented the cellular effects induced by WT-LPS EVs, thereby confirming the role of WT-LPS EVs on barrier disruption and macrophage inflammatory phenotype (Fig. 7c, d). There was no significant difference in the cellular activity of control EVs in presence or absence of EV uptake inhibitors (Fig. 7c, d).

To determine if the EVs carried residual LPS that caused the observed cellular effects, we measured endotoxin content in EVs using an Endotoxin detection kit (Thermo Fisher, Waltham, MA, USA). The endotoxin levels in EVs were almost negligible (less than 0.01 endotoxin units) in both saline and LPS-treated groups ruling out the possibility of LPS contamination (Fig. 7e). In addition, the lipid mediator 13-HODE (most abundant lipid mediator found in WT-LPS EVs) alone disrupted al-

veolar epithelial barrier function in a dose-dependent manner (Fig. 7f). In summary, the EV carried lipid mediators regulate alveolar epithelial and macrophage cell function during ALI.

Discussion

Considerable research dedicated to EVs is based on their miR and protein cargo [38–40]. However, much less is known about EVs' lipid and eicosanoid constituents generated from the cellular fatty acids. It is well-documented that lipid mediators control the initiation and resolution of acute lung inflammation, at least in part [6, 41, 42]. In the current study, we demonstrated that LPS-induced ALI increases the release of EVs into alveolar space, which carry a diverse array of ω-6 and ω-3 PUFA-derived lipid mediators and the total phospholipid content of EVs was significantly higher than that of EV-depleted BALF (Figs. 1, 2). Our data show that intranasal delivery of LPS (4 mg/kg) in mice induces acute neutrophilic lung inflammation along with the increased release of EVs into the alveolar space. Lung macrophages, alveo-

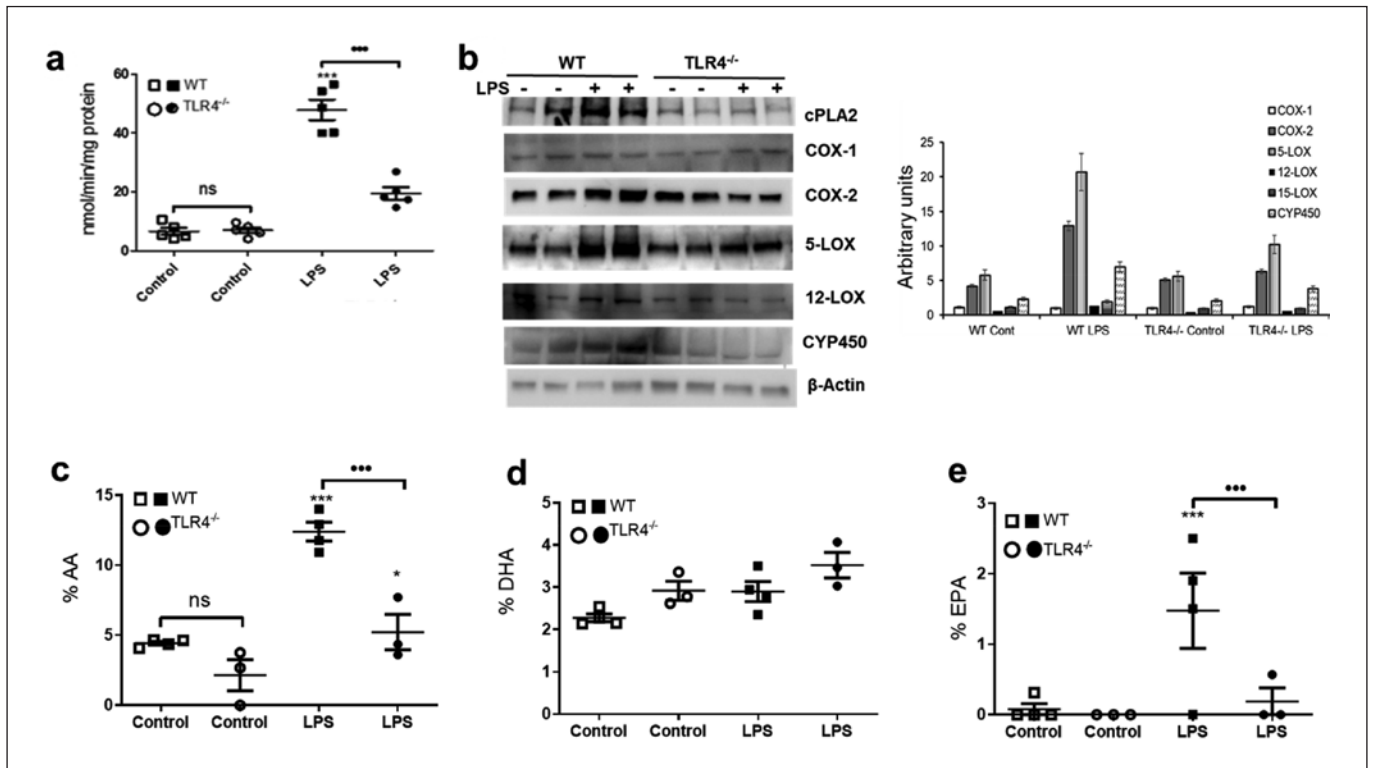


Fig. 6. Eicosanoids in EVs correlate with expression levels FA metabolic proteins and ω -6 and ω -3 fatty acid composition of lung macrophages. Total lung macrophages were isolated from saline and LPS-treated WT and TLR4^{-/-} mice. **a** Specific activity of cPLA2 measured by hydrolysis of μ mol of Arachidonoyl Thio-PC hydrolyzed per min per mg cellular protein. **b** Expression levels of cPLA2, COX-1, COX-2, 5-LOX, 12-LOX, CYP450, and β -actin and arbitrary densitometric units of COX-1, COX-2, 5-LOX,

12/15-LOX, CYP450, and β -actin averaged from different bots, $n = 8$ mice in each group, each well corresponds to lung macrophages pooled from two mice. In addition, total lipids were extracted from saline and LPS-treated mouse lung macrophages and analyzed by HPLC, **(c)** % AA **(d)** % DHA **(e)** % EPA. Statistical difference calculated by one-way ANOVA with Bonferroni correction. **a, c, e** *** $p \leq 0.001$ WT LPS versus WT-saline control, *** $p \leq 0.001$ WT-LPS versus TLR4^{-/-}-LPS.

lar epithelial cells, and neutrophils significantly contributed to the EV populations in BALF (Fig. 3e). BALF EVs of the LPS-challenged WT mice contained increased amounts of AA, DHA, and EPA-derived metabolites, which were either attenuated or undetectable in the LPS-challenged TLR4^{-/-} mice (Figs. 4, 5).

Previous studies have reported that eicosanoids have a short life in circulation or pulmonary edema fluid after their generation [43–45]. In contrast, recent studies suggest that the bilayer lipid membrane enclosing EVs is rich in sphingomyelin, cholesterol, phosphatidylserine, and glycosphingolipids compared to their parent cells, offering more structural stability compared to the plasma membrane, indicating the stability of lipid cargo carried in them [20]. We demonstrate that EVs carry diverse bioactive lipid mediators during ALI (Fig. 2). Specifically, the levels of pro-inflammatory and pro-resolution eico-

sanoids and ω -3 PUFA-released lipid mediators increased with LPS treatment during the acute-inflammatory phase, which reached basal levels by 15 days, coinciding with the resolution phase of LPS-induced ALI. Mammalian LOX enzymes are activated in pathological settings that initiate inflammation and tissue damage [46–48]. Different LOX metabolites of AA, including 5-HETE, 12-HETE, and 15-HETE, regulate the pathophysiology of lung diseases [49–51]. Thus, the HETEs packaged in EVs probably exert diverse cellular effects during inflammation and resolution phases of ALI pathophysiology. Monocytes and macrophages were shown to express the highest levels of 12/15-LOX, the enzyme responsible for generating 12-HETE in mice [52]. Twelve-HETE plays a pivotal role in inflammation by acting as a potent, pro-inflammatory chemoattractant for neutrophils, altering endothelial cell cytoskeleton

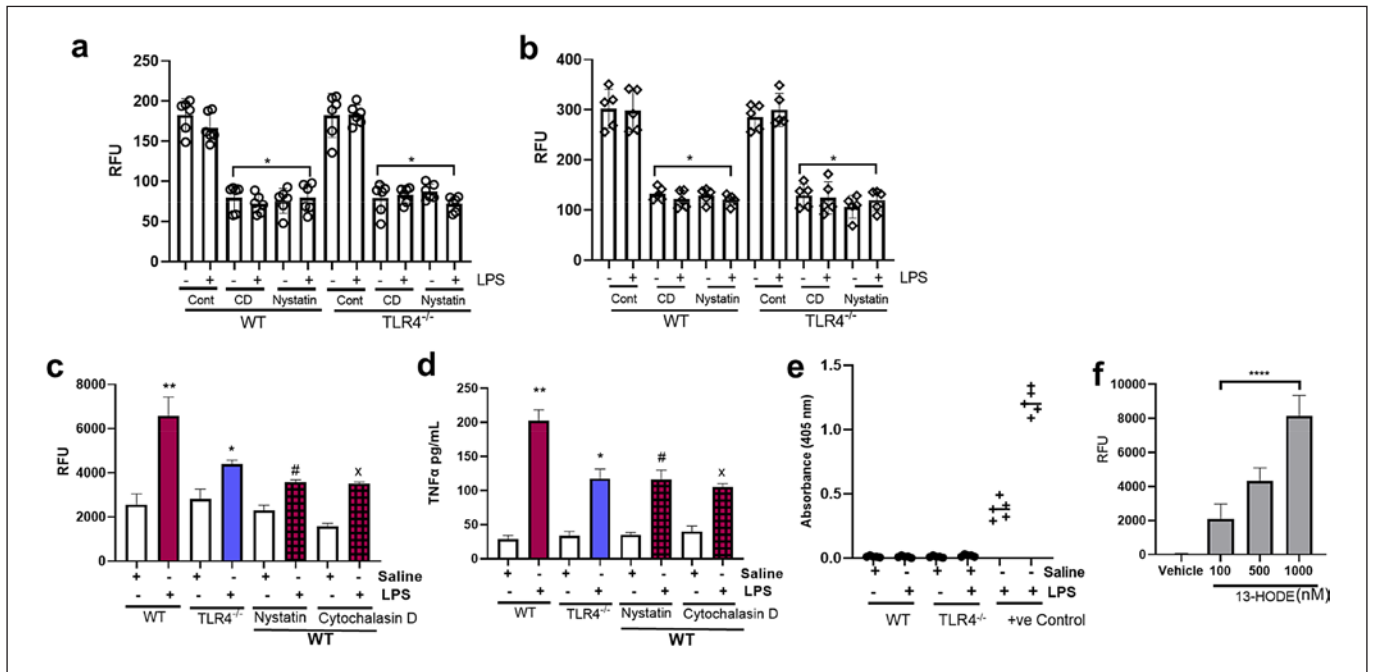


Fig. 7. BALF EVs alter alveolar epithelial and pulmonary macrophage function. **a** Alveolar epithelial cells and **b** lung macrophages were grown in the presence of PKH26-labeled EVs from WT, TLR4^{-/-}, solvent control (Cont), Cytochalasin (CD –10 µg/mL) or Nystatin (50 µg/mL) for 16 h and washed with 1X HBSS as described in methods. EV uptake was measured as RFU. **c** EVs from WT and TLR4^{-/-} mice, and 10 kDa FITC-dextran were added to 100% confluent monolayer of alveolar epithelial cells grown on transwells. After 16 h, flux of FITC-dextran to the bottom wells of the cell culture plate was measured at 492/520 nm. **d** EVs were added to lung macrophages grown in 96-well plates, and after 16 h, the release of TNF-α into the cell culture medium was measured. **e** Endotoxin contamination in EV preparation was determined by

the Pierce Endotoxin Detection kit. **f** 13-HODE (100–1,000 nM) and 10 kDa FITC-dextran were added to 100% confluent monolayer of alveolar epithelial cells grown on transwells. After 16 h, flux of FITC-dextran to the bottom wells of the cell culture plate was measured at 492/520 nm. Statistical difference calculated by one-way ANOVA with Bonferroni correction. **a, b** * $p \leq 0.01$ CD or Nystatin uptake versus Solvent control uptake of WT or TLR4^{-/-} EVs. **c, d** ** $p \leq 0.01$ WT LPS EVs versus WT-saline EVs, * $p \leq 0.05$ WT-LPS versus TLR4^{-/-}-LPS EVs, # $p \leq 0.05$ WT-LPS EVs versus WT-LPS + Nystatin, and x $p \leq 0.05$ WT-LPS EVs versus WT-LPS + CD pretreated alveolar epithelial cells. **f** **** $p \leq 0.0001$ 13-HODE-treated alveolar epithelial cells versus vehicle-treated cells.

and expression of adhesion molecules [51, 53–55]. Interestingly, DHA and AA-derived pro-resolution mediators, including Resolvin D6, 8oxo resolvin D1, Maresin1, and Lipoxin A4, were detected in EVs released during LPS-induced ALI (Fig. 2). The beneficial effects of resolvins in immunomodulation and actively resolving inflammation in different organ systems are well established [56–59]. For example, in a study using human vascular endothelial cells, Resolvin D1 reverted LPS-induced tight junctional disruption and the increase of cellular permeability by regulating I κBα signaling [60]. More importantly, analysis of AA metabolites in sepsis-induced ARDS patient plasma revealed that non-survivors had significantly higher prostaglandin F2 and LTB4 [61]. In addition, the ARDS patient plasma had elevated levels of the pro-resolution mediators, resolvin E1, resolvin D5,

and 17r-protectin D1, that persisted along with pro-inflammatory mediators until 7 days in these patients, similar to our observation in the mouse ALI model. Thus, the EVs likely carried a significant proportion of the total plasma eicosanoids reported in this study. Furthermore, 15-LOX metabolites of linoleic acid 13-HODE and its oxidation product 13-OxoODE were also detected in EVs (Fig. 2). Although the role of these oxidation products has not been investigated in detail, published reports demonstrate that 13-HODE negatively regulates endothelial barrier integrity and causes endothelial cell apoptosis [62]. Moreover, the oxidized LA metabolites and their derivatives (9-HODE, 13-HODE, 9-oxoODE, 13-oxoODE) have been linked to cardiovascular inflammation [63]. Thus, Oxidized LA metabolites transported through the EV could cause pulmonary microvascular

barrier dysfunction in the LPS-induced ALI mice [64]. Similarly, activation TLRs and purinergic receptor PY27 were reported to induce inflammasome formation and concurrent triggering of lipoxin synthesis in macrophages [65]. This study suggested that inflammasome formation also triggers an eicosanoid storm that contains both pro-inflammatory and proresolving lipid mediators.

Our previous studies and others have established a pivotal role for pulmonary macrophages in regulating the LPS and abdominal sepsis-induced ALI severity in mouse models [33, 66–68]. Therefore, we sought to determine if the differences in EV eicosanoids correlate with the alveolar macrophage PUFA composition and the PUFA metabolizing enzymes. Alveolar macrophages from LPS-treated WT mice showed an increased % of AA and EPA compared to LPS-treated TLR4^{-/-} mice (Fig. 6). In addition, the enzymatic activity of cPLA2, expression levels of COX-2, 5-LOX, and CYP P450 proteins were lower in TLR4^{-/-} lung macrophages while COX-1 remained the same (Fig. 6). Thus, expression levels of PUFA metabolizing enzymes in lung macrophages align with the lipid mediators in EVs. In addition to the lipid mediators identified in the current study, miRs (miR-466, miR-223/142, miR-17, miR-221, miR-92a-3p), the inflammatory cytokine TNF- α , and the microvesicular Caspase 1 were implicated in the regulation of the ALI [25–27, 29, 69]. Therefore, it appears that EVs deliver a cargo of proteins, miRs, and PUFA metabolites that regulate cellular function during ALI pathophysiology.

In summary, our study demonstrates for the first time that the EVs carry a diverse array of lipid mediators, which can modulate the alveolar epithelial cell barrier and lung macrophage inflammatory phenotype during ALI (Fig. 7). PUFA metabolite profile depends on the inflammatory phenotype of the alveolar macrophages and their interaction with other lung cells. However, the eicosanoid and lipid mediator synthesis is a much complex process involving eicosanoid class switching and transcellular synthesis of some lipoxins, in addition to other regulatory cell-signaling mechanisms. Future studies are required to delineate the individual role of EV proteins, miRs, and lipids in regulating ALI/ARDS pathophysiology.

Statement of Ethics

This study protocol was reviewed and approved by the Institutional Animal Care and Use Committee (IACUC) of The Ohio State University, approval number 2013A00000105-R1.

Conflict of Interest Statement

The authors have declared that no conflict of interest exists.

Funding Sources

This study was supported by the American Heart Association Grant 17SDG33410982 to M.K., National Institutes of Health HL137224 to J.W.C. and National Center for Research Resources (in part), and National Institutes of Health Grant S10RR027926 to K.R.M. TEM Images presented in this report were generated using the instruments and services at the Campus Microscopy and Imaging Facility, The Ohio State University. This facility is supported in part by Grant P30 CA016058, National Cancer Institute, Bethesda, MD, USA, and OSU flow cytometry analysis is supported by P30CA016058. The OSU Mass spectrometry and Proteomics facility are supported by NIH Award Number Grant P30 CA016058 and Fusion Orbitrap instrument by NIH Award Number Grant S10 OD018056.

Author Contributions

M.K., N.P., and J.W.C. conceived the project. T.S.N. carried out the mouse ALI experiments, E.V. isolations, N.T.A. nanoparticle analysis, and cytokine measurements. Lipidomics data were generated with help from K.R.M. S.R.K., A.Y., and N.P. analyzed the macrophage fatty acid composition. B.F.R. and S.C. analyzed the lung macrophages. M.K. carried out mouse ALI experiments, analyzed data, and wrote the manuscript.

Data Availability Statement

All data generated or analyzed during this study are included in this article and its online supplementary material files. Further inquiries can be directed to the corresponding author.

References

- 1 Matthay MA, Zemans RL, Zimmerman GA, Arabi YM, Beitler JR, Mercat A, et al. Acute respiratory distress syndrome. *Nat Rev Dis Primers*. 2019;5(1):18.
- 2 Bos LDJ, Artigas A, Constantin JM, Hagens LA, Heijnen N, Laffey JG, et al. Precision medicine in acute respiratory distress syndrome: workshop report and recommendations for future research. *Eur Respir Rev*. 2021;30(159):200317.
- 3 Matthay MA, Zemans RL. The acute respiratory distress syndrome: pathogenesis and treatment. *Annu Rev Pathol*. 2011;6:147–63.
- 4 Herrero R, Rojas Y, Esteban A. Novel pharmacologic approaches for the treatment of ARDS. In: Vincent JL, editor. *Annual update in intensive care and emergency medicine 2014*. Cham: Springer International Publishing; 2014. p. 231–43.

- 5 Christman JW, Karpurapu M, Pei D. Can acute respiratory distress syndrome be treated? *Future Med Chem*. 2021;13(8):687–90.
- 6 Bonnans C, Levy BD. Lipid mediators as agonists for the resolution of acute lung inflammation and injury. *Am J Respir Cell Mol Biol*. 2007;36(2):201–5.
- 7 Wei J, Gronert K. Eicosanoid and specialized proresolving mediator regulation of lymphoid cells. *Trends Biochem Sci*. 2019;44(3):214–25.
- 8 Yonker LM, Barrios J, Mou H, Hurley BP. Untapped potential: therapeutically targeting eicosanoids and endocannabinoids in the lung. *Clin Pharmacol Ther*. 2021.
- 9 Nagase T, Uozumi N, Ishii S, Kume K, Izumi T, Ouchi Y, et al. Acute lung injury by sepsis and acid aspiration: a key role for cytosolic phospholipase A2. *Nat Immunol*. 2000;1(1):42–6.
- 10 Nagase T, Uozumi N, Aoki-Nagase T, Terawaki K, Ishii S, Tomita T, et al. A potent inhibitor of cytosolic phospholipase A2, arachidonyl trifluoromethyl ketone, attenuates LPS-induced lung injury in mice. *Am J Physiol Lung Cell Mol Physiol*. 2003;284(5):L720–6.
- 11 Kitsiouli E, Nakos G, Lekka ME. Phospholipase A2 subclasses in acute respiratory distress syndrome. *Biochim Biophys Acta*. 2009;1792(10):941–53.
- 12 Hanna VS, Hafez EAA. Synopsis of arachidonic acid metabolism: a review. *J Adv Res*. 2018;11:23–32.
- 13 Serhan CN. Discovery of specialized pro-resolving mediators marks the dawn of resolution physiology and pharmacology. *Mol Aspects Med*. 2017;58:1–11.
- 14 Chiang N, Serhan CN. Structural elucidation and physiologic functions of specialized pro-resolving mediators and their receptors. *Mol Aspects Med*. 2017;58:114–29.
- 15 Serhan CN. Systems approach to inflammation resolution: identification of novel anti-inflammatory and pro-resolving mediators. *J Thromb Haemost*. 2009;7(Suppl 1):44–8.
- 16 Folco G, Murphy RC. Eicosanoid transcellular biosynthesis: from cell-cell interactions to in vivo tissue responses. *Pharmacol Rev*. 2006;58(3):375–88.
- 17 Vidal M. Exosomes: revisiting their role as “garbage bags”. *Traffic*. 2019;20(11):815–28.
- 18 Hessvik NP, Llorente A. Current knowledge on exosome biogenesis and release. *Cell Mol Life Sci*. 2018;75(2):193–208.
- 19 Russell AE, Sneider A, Witwer KW, Bergese P, Bhattacharyya SN, Cocks A, et al. Biological membranes in EV biogenesis, stability, uptake, and cargo transfer: an ISEV position paper arising from the ISEV membranes and EVs workshop. *J Extracell Vesicles*. 2019;8(1):1684862.
- 20 Record M, Carayon K, Poirot M, Silvente-Poirot S. Exosomes as new vesicular lipid transporters involved in cell-cell communication and various pathophysiological. *Biochim Biophys Acta*. 2014;1841(1):108–20.
- 21 Lee H, Zhang D, Zhu Z, Dela Cruz CS, Jin Y. Epithelial cell-derived microvesicles activate macrophages and promote inflammation via microvesicle-containing microRNAs. *Sci Rep*. 2016;6(1):35250.
- 22 Haggadone MD, Peters-Golden M. Microenvironmental influences on extracellular vesicle-mediated communication in the lung. *Trends Mol Med*. 2018;24(11):963–75.
- 23 Yuan Z, Petree JR, Lee FE, Fan X, Salaita K, Guidot DM, et al. Macrophages exposed to HIV viral protein disrupt lung epithelial cell integrity and mitochondrial bioenergetics via exosomal microRNA shuttling. *Cell Death Dis*. 2019;10(8):580.
- 24 Boilard E. Extracellular vesicles and their content in bioactive lipid mediators: more than a sack of microRNA. *J Lipid Res*. 2018;59(11):2037–46.
- 25 Shikano S, Gon Y, Maruoka S, Shimizu T, Kozu Y, Iida Y, et al. Increased extracellular vesicle miRNA-466 family in the bronchoalveolar lavage fluid as a precipitating factor of ARDS. *BMC Pulm Med*. 2019;19(1):110.
- 26 Zhang D, Lee H, Wang X, Groot M, Sharma L, Dela Cruz CS, et al. A potential role of microvesicle-containing miR-223/142 in lung inflammation. *Thorax*. 2019;74(9):865–74.
- 27 Lee H, Zhang D, Wu J, Otterbein LE, Jin Y. Lung epithelial cell-derived microvesicles regulate macrophage migration via MicroRNA-17/221-induced integrin β 1 recycling. *J Immunol*. 2017;199(4):1453–64.
- 28 Liu F, Peng W, Chen J, Xu Z, Jiang R, Shao Q, et al. Exosomes derived from alveolar epithelial cells promote alveolar macrophage activation mediated by miR-92a-3p in sepsis-induced acute lung injury. *Front Cell Infect Microbiol*. 2021;11:646546.
- 29 Soni S, Wilson MR, O’Dea KP, Yoshida M, Katbeh U, Woods SJ, et al. Alveolar macrophage-derived microvesicles mediate acute lung injury. *Thorax*. 2016;71(11):1020–9.
- 30 Nie Y, Nirujogi TS, Ranjan R, Reader BF, Chung S, Ballinger MN, et al. PolyADP-ribosylation of NFATc3 and NF-kappaB transcription factors modulate macrophage inflammatory gene expression in LPS-induced acute lung injury. *J Innate Immun*. 2020;1–11.
- 31 Thery C, Amigorena S, Raposo G, Clayton A. Isolation and characterization of exosomes from cell culture supernatants and biological fluids. *Curr Protoc Cell Biol*. 2006.
- 32 Norris PC, Skulas-Ray AC, Riley I, Richter CK, Kris-Etherton PM, Jensen GL, et al. Identification of specialized pro-resolving mediator clusters from healthy adults after intravenous low-dose endotoxin and omega-3 supplementation: a methodological validation. *Sci Rep*. 2018;8(1):18050.
- 33 Karpurapu M, Lee YG, Qian Z, Wen J, Ballinger MN, Rusu L, et al. Inhibition of nuclear factor of activated T cells (NFAT) c3 activation attenuates acute lung injury and pulmonary edema in murine models of sepsis. *OncoTarget*. 2018;9(12):10606–20.
- 34 Sherwani SI, Pabon S, Patel RB, Sayyid MM, Hagele T, Kotha SR, et al. Eicosanoid signaling and vascular dysfunction: methylmercury-induced phospholipase D activation in vascular endothelial cells. *Cell Biochem Biophys*. 2013;67(2):317–29.
- 35 Zemans RL, Henson PM, Henson JE, Janssen WJ. Conceptual approaches to lung injury and repair. *Ann Am Thorac Soc*. 2015;12(Suppl 1):S9–15.
- 36 Hoshino K, Takeuchi O, Kawai T, Sanjo H, Ogawa T, Takeda Y, et al. Cutting edge: toll-like receptor 4 (TLR4)-deficient mice are hyporesponsive to lipopolysaccharide: evidence for TLR4 as the Lps gene product. *J Immunol*. 1999;162(7):3749–52.
- 37 Poltorak A, Smirnova I, He X, Liu MY, Van Huffel C, McNally O, et al. Genetic and physical mapping of the Lps locus: identification of the toll-4 receptor as a candidate gene in the critical region. *Blood Cells Mol Dis*. 1998;24(3):340–55.
- 38 Wisler JR, Singh K, McCarty AR, Abouhashem ASE, Christman JW, Sen CK. Proteomic pathway analysis of monocyte-derived exosomes during surgical sepsis identifies immunoregulatory functions. *Surg Infect*. 2020;21(2):101–11.
- 39 Draijer C, Speth JM, Penke LRK, Zaslona Z, Bazzill JD, Lugogo N, et al. Resident alveolar macrophage-derived vesicular SOCS3 dampens allergic airway inflammation. *FASEB J*. 2020;34(3):4718–31.
- 40 Weber B, Franz N, Marzi I, Henrich D, Leppik L. Extracellular vesicles as mediators and markers of acute organ injury: current concepts. *Eur J Trauma Emerg Surg*. 2021.
- 41 Ott J, Hiesgen C, Mayer K. Lipids in critical care medicine. *Prostaglandins Leukot Essent Fatty Acids*. 2011;85(5):267–73.
- 42 Robb CT, Regan KH, Dorward DA, Rossi AG. Key mechanisms governing resolution of lung inflammation. *Semin Immunopathol*. 2016;38(4):425–48.
- 43 Matthay MA, Eschenbacher WL, Goetzl EJ. Elevated concentrations of leukotriene D4 in pulmonary edema fluid of patients with the adult respiratory distress syndrome. *J Clin Immunol*. 1984;4(6):479–83.
- 44 Ratnoff WD, Matthay MA, Wong MY, Ito Y, Vu KH, Wiener-Kronish J, et al. Sulfidopeptide-leukotriene peptidases in pulmonary edema fluid from patients with the adult respiratory distress syndrome. *J Clin Immunol*. 1988;8(4):250–8.
- 45 von Moltke J, Trinidad NJ, Moayeri M, Kintzer AF, Wang SB, van Rooijen N, et al. Rapid induction of inflammatory lipid mediators by the inflammasome in vivo. *Nature*. 2012;490(7418):107–11.
- 46 Taylor-Fishwick DA, Weaver J, Glenn L, Kuhn N, Rai G, Jadhav A, et al. Selective inhibition of 12-lipoxygenase protects islets and beta cells from inflammatory cytokine-mediated beta cell dysfunction. *Diabetologia*. 2015;58(3):549–57.

- 47 Kuhn H, Banthiya S, van Leyen K. Mammalian lipoxygenases and their biological relevance. *Biochim Biophys Acta*. 2015;1851(4):308–30.
- 48 Mahboubi-Rabbani M, Zarghi A. Lipoxygenase inhibitors as cancer chemopreventives: discovery, recent developments, and future perspectives. *Curr Med Chem*. 2019.
- 49 Awwad K, Steinbrink SD, Fromel T, Lill N, Isaak J, Hafner AK, et al. Electrophilic fatty acid species inhibit 5-lipoxygenase and attenuate sepsis-induced pulmonary inflammation. *Antioxid Redox Signal*. 2014;20(17):2667–80.
- 50 Schultz D, Methling K, KoInfekt Study G, Rothe M, Lalk M. Eicosanoid profile of influenza A virus infected pigs. *Metabolites*. 2019;9(7):130.
- 51 Rossaint J, Nadler JL, Ley K, Zarbock A. Eliminating or blocking 12/15-lipoxygenase reduces neutrophil recruitment in mouse models of acute lung injury. *Crit Care*. 2012;16(5):R166.
- 52 Huo Y, Zhao L, Hyman MC, Shashkin P, Harry BL, Burcin T, et al. Critical role of macrophage 12/15-lipoxygenase for atherosclerosis in apolipoprotein E-deficient mice. *Circulation*. 2004;110(14):2024–31.
- 53 Cunningham FM, Woollard PM. 12(R)-hydroxy-5,8,10,14-eicosatetraenoic acid is a chemoattractant for human polymorphonuclear leucocytes in vitro. *Prostaglandins*. 1987;34(1):71–8.
- 54 Tang DG, Timar J, Grossi IM, Renaud C, Kimler VA, Diglio CA, et al. The lipoxygenase metabolite, 12(S)-HETE, induces a protein kinase C-dependent cytoskeletal rearrangement and retraction of microvascular endothelial cells. *Exp Cell Res*. 1993;207(2):361–75.
- 55 Bolick DT, Orr AW, Whetzel A, Srinivasan S, Hatley ME, Schwartz MA, et al. 12/15-lipoxygenase regulates intercellular adhesion molecule-1 expression and monocyte adhesion to endothelium through activation of RhoA and nuclear factor-kappaB. *Arterioscler Thromb Vasc Biol*. 2005;25(11):2301–7.
- 56 Abdunour RE, Dalli J, Colby JK, Krishnamoorthy N, Timmons JY, Tan SH, et al. Maresin 1 biosynthesis during platelet-neutrophil interactions is organ-protective. *Proc Natl Acad Sci U S A*. 2014;111(46):16526–31.
- 57 Haworth O, Levy BD. Endogenous lipid mediators in the resolution of airway inflammation. *Eur Respir J*. 2007;30(5):980–92.
- 58 Hecker M, Linder T, Ott J, Walmrath HD, Lohmeyer J, Vadasz I, et al. Immunomodulation by lipid emulsions in pulmonary inflammation: a randomized controlled trial. *Crit Care*. 2015;19:226.
- 59 Fang X, Abbott J, Cheng L, Colby JK, Lee JW, Levy BD, et al. Human mesenchymal stem (Stromal) cells promote the resolution of acute lung injury in part through lipoxin A4. *J Immunol*. 2015;195(3):875–81.
- 60 Zhang X, Wang T, Gui P, Yao C, Sun W, Wang L, et al. Resolvin D1 reverts lipopolysaccharide-induced TJ proteins disruption and the increase of cellular permeability by regulating I κ B α signaling in human vascular endothelial cells. *Oxid Med Cell Longev*. 2013;2013:185715.
- 61 Dalli J, Colas RA, Quintana C, Barragan-Bradford D, Hurwitz S, Levy BD, et al. Human sepsis eicosanoid and proresolving lipid mediator temporal profiles: correlations with survival and clinical outcomes. *Crit Care Med*. 2017;45(1):58–68.
- 62 Ryman VE, Packiriswamy N, Sordillo LM. Apoptosis of endothelial cells by 13-HPODE contributes to impairment of endothelial barrier integrity. *Mediators Inflamm*. 2016;2016:9867138.
- 63 Ramsden CE, Ringel A, Feldstein AE, Taha AY, MacIntosh BA, Hibbeln JR, et al. Lowering dietary linoleic acid reduces bioactive oxidized linoleic acid metabolites in humans. *Prostaglandins Leukot Essent Fatty Acids*. 2012;87(4–5):135–41.
- 64 Kobayashi K, Horikami D, Omori K, Nakamura T, Yamazaki A, Maeda S, et al. Thromboxane A2 exacerbates acute lung injury via promoting edema formation. *Sci Rep*. 2016;6:32109.
- 65 Norris PC, Gosselin D, Reichart D, Glass CK, Dennis EA. Phospholipase A2 regulates eicosanoid class switching during inflammasome activation. *Proc Natl Acad Sci U S A*. 2014;111(35):12746–51.
- 66 Steinmuller M, Srivastava M, Kuziel WA, Christman JW, Seeger W, Welte T, et al. Endotoxin induced peritonitis elicits monocyte immigration into the lung: implications on alveolar space inflammatory responsiveness. *Respir Res*. 2006;7:30.
- 67 Karpurapu M, Wang X, Deng J, Park H, Xiao L, Sadikot RT, et al. Functional PU.1 in macrophages has a pivotal role in NF-kappaB activation and neutrophilic lung inflammation during endotoxemia. *Blood*. 2011;118(19):5255–66.
- 68 Herold S, Mayer K, Lohmeyer J. Acute lung injury: how macrophages orchestrate resolution of inflammation and tissue repair. *Front Immunol*. 2011;2:65.
- 69 Sarkar A, Mitra S, Mehta S, Raices R, Wewers MD. Monocyte derived microvesicles deliver a cell death message via encapsulated caspase-1. *PLoS One*. 2009;4(9):e7140.